

Mean-field effects in the Galloway–Proctor flow

Karl-Heinz Rädler¹ and Axel Brandenburg² ^{*}

¹ *Astrophysical Institute Potsdam, An der Sternwarte 16, D-14482 Potsdam, Germany*

² *NORDITA, Roslagstullsbacken 23, SE - 106 91 Stockholm, Sweden*

ABSTRACT

The coefficients defining the mean electromotive force in a Galloway–Proctor flow are determined. This flow shows a two-dimensional pattern and is helical. The pattern wobbles in its plane. Apart from one exception a circular motion of the flow pattern is assumed. This corresponds to one of the cases considered recently by Courvoisier, Hughes and Tobias (2006, Phys. Rev. Lett., 96, 034503). An analytic theory of the α effect and related effects in this flow is developed within the second-order correlation approximation and a corresponding fourth-order approximation. In the validity range of these approximations there is an α effect but no γ effect, or pumping effect. Numerical results obtained with the test-field method, which are independent of these approximations, confirm the results for α and show that γ is in general nonzero. Both α and γ show a complex dependency on the magnetic Reynolds number and other parameters that define the flow, that is, amplitude and frequency of the wobbling motion. Some results for the magnetic diffusivity η_t and a related quantity are given, too. Finally a result for α in the case of a randomly varying flow without the aforementioned circular motion is presented. This flow may be a more appropriate model for studying the α effect and related effects in flows that are statistical isotropic in a plane.

Key words: magnetic fields — MHD — hydrodynamics – turbulence

1 INTRODUCTION

In the astrophysical context, turbulent flows, e.g. in stellar convection zones or in accretion discs and galaxies, are generally anisotropic and time-dependent. A simple model of a flow with such properties is that by Galloway & Proctor (1992). This flow is two-dimensional, depends only on two Cartesian coordinates, e.g. x and y , which can simplify the analysis significantly, even in dynamo problems that are inherently three-dimensional. The Galloway–Proctor (GP) flow is related to a flow considered by Roberts (1972). The Roberts flow¹ is an early example of a spatially periodic flow that produces an alpha effect. The alpha term in the averaged form of the induction equation is crucial to model the generation of large-scale magnetic fields from small-scale helical fluid motions in stars and galaxies; see, for example, Moffatt (1978), Parker (1979), and Krause & Rädler (1980) for standard references. However, unlike the Roberts flow, the GP flow is time-dependent with a flow pattern wobbling in the (x, y) plane in a circular fashion. Both the GP flow and the Roberts flow have a velocity component out of this plane such that the flow can be fully helical, i.e. the velocity is proportional to its curl.

Particularly important is the dependence of the α effect on the magnetic Reynolds number, R_m . While for the Roberts flow α declines with R_m in the large R_m limit, in the case of the GP flow

according to the results by Courvoisier, Hughes & Tobias (2006) (in the following referred to as CHT06) and Courvoisier (2008) there is a more complicated dependence on R_m with sign changes and no indication of convergence with increasing R_m .

In many studies turbulent astrophysical flows have been modelled by random forcing. In the case of helical isotropic turbulence such investigations show that α approaches a finite value as soon as R_m exceeds a value of the order of unity. This has been observed at least for Reynolds numbers up to 200 (Sur et al. 2008).

The purpose of this paper is to study the effects of the GP flow in more detail in order to understand the influence of time-dependence and anisotropy on the value of α and other turbulent transport coefficients. In particular, it is important to document the differences and similarities with turbulent flows that are statistically isotropic and irregular in space and time. We focus attention here on the simplest case considered in CHT06 with a flow being purely periodic in time and add a few results for a simple flow with random time dependence.

A number of similarities, but also some striking differences between turbulent flows and the Roberts flow are known. Similar in both flows is the fact that there is an α effect whose magnitude increases with R_m as long as the latter does not exceed some value in the order of unity. However, for larger R_m , the α coefficient in isotropic turbulence settles to a constant value (Sur et al. 2008), while for the Roberts flow α tends to zero as $R_m \rightarrow \infty$ (Soward 1987, 1989; Rädler et al. 2002a,b). Furthermore, there is no γ effect, or pumping effect, neither for isotropic turbulence nor for the

^{*} E-mail: khraedler@arcor.de (KHR); brandenb@nordita.org (AB)

¹ As usual, the term Roberts flow refers to the flow given by equation (5.1) of Roberts (1972).

Roberts flow. On the other hand, in the time-dependent GP flow γ effects have been reported (CHT06). A γ effect corresponds to antisymmetric contributions of the α tensor. This raises the question about the possible existence of antisymmetric contributions to the turbulent magnetic diffusivity tensor, or η_t tensor.

These aspects are now straightforward to address using the recently developed test-field method to calculate numerically all components of the α and η_t tensors defining the mean electromotive force $\overline{\mathcal{E}}$ for a given flow field (Schinnerer et al. 2005, 2007). If, as we assume here, too, the mean magnetic field $\overline{\mathbf{B}}$ depends only on one of the Cartesian coordinates, say z , only two 2×2 tensors for α and η_t are of interest. The test-field method has recently been used to calculate diagonal and off-diagonal components of η_t (Brandenburg et al. 2008), the magnetic Reynolds number dependence of α and η_t (Sur et al. 2008), as well as their scale dependence (Brandenburg, Rädler & Schinnerer 2008). We begin by exploring general properties of the mean electromotive force in the GP flow and present analytical results for coefficients like α and γ , which are crucial for the electromotive force, gained in the second-order correlation approximation and in a corresponding fourth-order approximation. After explaining the test-field method we give a series of numerical results for such coefficients, which are independent of approximations of that kind, and discuss them in detail.

2 MEAN-FIELD ELECTRODYNAMICS WITH GALLOWAY-PROCTOR FLOW

2.1 Definition of the problem

Consider a magnetic field \mathbf{B} in an infinitely extended homogeneous conducting fluid with constant magnetic diffusivity η moving with a velocity \mathbf{u} . Its behavior is governed by

$$\partial_t \mathbf{B} - \eta \nabla^2 \mathbf{B} - \nabla \times (\mathbf{u} \times \mathbf{B}) = \mathbf{0}, \quad \nabla \cdot \mathbf{B} = 0. \quad (1)$$

Referring to a Cartesian coordinate system (x, y, z) the velocity \mathbf{u} is specified by

$$\mathbf{u} = -\hat{z} \times \nabla \psi - \hat{z} k_H \mathbf{b} \quad (2)$$

with

$$\psi = \frac{u_0}{k_H} [\cos(k_H x + \varphi_x) + \cos(k_H y + \varphi_y)]. \quad (3)$$

Here \hat{z} means the unit vector in the z direction, k_H is a positive constant such that $2\pi/k_H$ is the length of the diagonal of a flow cell, and φ_x and φ_y are functions of time to be specified later. Further we have $u_0 = u_{\text{rms}}/\sqrt{2}$. In the special case $\varphi_x = \varphi_y = 0$ the flow agrees with a Roberts flow. For non-zero φ_x or φ_y a properly moving frame of reference can be found in which we have again a steady Roberts flow pattern. In our original frame each point of this pattern moves with the velocity $-k_H^{-1}(\partial_t \varphi_x, \partial_t \varphi_y)$ in the xy plane. In (2) the ratio of the flow components in the xy plane and in z direction has been fixed such that the modulus of the average of the kinetic helicity $\mathbf{u} \cdot (\nabla \times \mathbf{u})$ over all x and y for given u_0 takes its maximum. With the signs chosen this average is equal to $-2u_0^2 k_H$.

In view of the first example treated in CHT06 we specify the flow generally defined by (2) and (3) further to be a Galloway-Proctor flow and put

$$\varphi_x = \epsilon \cos \omega t, \quad \varphi_y = \epsilon \sin \omega t, \quad (4)$$

where ϵ and ω are considered as non-negative constants. We label this flow in what follows by (i). Each point of this pattern moves with the frequency $\omega/2\pi$ on a circle with the radius ϵ/k_H .

To come closer to a turbulent situation CHT06 added a random function of time to the arguments ωt in (4). Another case of some interest occurs if we simply interpret φ_x and φ_y as random functions. More precisely we put

$$\varphi_x = \epsilon \phi_x(t/\tau_c), \quad \varphi_y = \epsilon \phi_y(t/\tau_c), \quad (5)$$

where ϵ is again a constant, ϕ_x and ϕ_y are two independent but statistically equivalent random functions, which take positive and negative values between -1 and 1 and tend to zero with growing moduli of the argument, and τ_c is some correlation time. We label this random flow by (ii).

2.2 Mean-field concept

Adopting the mean-field concept, we denote mean fields by an overbar and define them as averages over all x and y . We have then $\overline{\mathbf{u}} = \mathbf{0}$. Taking the average of (1) we find

$$\partial_t \overline{\mathbf{B}} - \eta \nabla^2 \overline{\mathbf{B}} - \nabla \times \overline{\mathcal{E}} = \mathbf{0}, \quad \nabla \cdot \overline{\mathbf{B}} = 0, \quad (6)$$

with the mean electromotive force

$$\overline{\mathcal{E}} = \overline{\mathbf{u} \times \mathbf{b}}, \quad (7)$$

where $\mathbf{b} = \mathbf{B} - \overline{\mathbf{B}}$. [In (6) ∇ reduces simply to $(0, 0, \partial_z)$.] From (1) and (6) we conclude that \mathbf{b} has to obey

$$(\partial_t - \eta \nabla^2) \mathbf{b} = (\overline{\mathbf{B}} \cdot \nabla) \mathbf{u} - (\mathbf{u} \cdot \nabla) \overline{\mathbf{B}} + \nabla \times (\mathbf{u} \times \mathbf{b} - \overline{\mathbf{u} \times \mathbf{b}}), \quad \nabla \cdot \mathbf{b} = 0. \quad (8)$$

We adopt here the assumption that the mean electromotive force $\overline{\mathcal{E}}$ is, apart from \mathbf{u} and η , completely determined by $\overline{\mathbf{B}}$ and its first spatial derivatives. (This assumption will be relaxed in Sect. 4.) This implies that there is no small-scale dynamo and that sufficient time has elapsed since the initial instant so that $\overline{\mathcal{E}}$ no longer depends on any initial conditions. Since $\overline{\mathbf{B}}$ is by definition independent of x and y its spatial derivatives can be represented by $\nabla \times \overline{\mathbf{B}}$. We write simply $\overline{\mathcal{J}}$ instead of $\nabla \times \overline{\mathbf{B}}$, being aware that the mean electric current density is really $\nabla \times \overline{\mathbf{B}}/\mu$ (rather than $\overline{\mathcal{J}}$), where μ is magnetic permeability of the conducting fluid. Clearly we have now $\overline{\mathcal{J}} = (-\partial \overline{B}_y / \partial z, \partial \overline{B}_x / \partial z, 0)$. For the sake of simplicity we further assume that $\overline{\mathbf{B}}$ is steady. In the so defined framework we may write

$$\overline{\mathcal{E}}_i = \alpha_{ij} \overline{B}_j - \eta_{ij} \overline{\mathcal{J}}_j \quad (9)$$

with tensors α_{ij} and η_{ij} determined by \mathbf{u} and η only. Both α_{ij} and η_{ij} , and so $\overline{\mathcal{E}}_i$, too, depend in general on time.

We see from (8) that, if $\overline{\mathbf{B}}$ is a uniform field, \mathbf{b} and therefore $\overline{\mathcal{E}}$ are independent of \overline{B}_z . Hence we have $\alpha_{i3} = 0$. Furthermore, since $\overline{\mathcal{J}}_z = 0$, clearly η_{i3} is without interest, and we put $\eta_{i3} = 0$.

2.3 Mean electromotive force in case (i)

For a more detailed investigation of $\overline{\mathcal{E}}$ we focus on the fluid flow of type (i). In this case α_{ij} and η_{ij} are periodic in time with a basic period equal to that of \mathbf{u} , that is $2\pi/\omega$, or (as we will see below) a fraction of it.

Remarkably the velocity field $\mathbf{u} = \mathbf{u}(x, y, t)$ defined by (2), (3) and (4) is invariant under a 90° rotation about the z axis and a simultaneous retarding by $\pi/2\omega$ (that is, $\omega t \rightarrow \omega t - \pi/2$). Consequently the α_{ij} in the correspondingly rotated coordinate system, which we denote by α'_{ij} , have to satisfy the relation

$$\alpha'_{ij}(t - \pi/2\omega) = \alpha_{ij}(t). \quad (10)$$

If we consider for a moment the change of the spatial coordinate system only and ignore any time dependence we have $\alpha'_{11} = \alpha_{22}$, $\alpha'_{12} = -\alpha_{21}$, $\alpha'_{21} = -\alpha_{12}$, $\alpha'_{22} = \alpha_{11}$, $\alpha'_{31} = -\alpha_{32}$ and $\alpha'_{32} = \alpha_{31}$. Hence (10) provides us with

$$\begin{aligned} \alpha_{11}(t) &= +\alpha_{22}(t - \pi/2\omega), & \alpha_{22}(t) &= +\alpha_{11}(t - \pi/2\omega), \\ \alpha_{12}(t) &= -\alpha_{21}(t - \pi/2\omega), & \alpha_{21}(t) &= -\alpha_{12}(t - \pi/2\omega), \\ \alpha_{31}(t) &= -\alpha_{32}(t - \pi/2\omega), & \alpha_{32}(t) &= +\alpha_{31}(t - \pi/2\omega). \end{aligned} \quad (11)$$

From the first two lines we conclude firstly that α_{11} , α_{12} , α_{21} and α_{22} have as functions of time a basic period of π/ω (not $2\pi/\omega$) and that $\alpha_{22}(t) = \alpha_{11}(t \pm \pi/2\omega)$ and $\alpha_{21}(t) = -\alpha_{12}(t \pm \pi/2\omega)$. The last line of (11) tells us that the averages of α_{31} and α_{32} over the period $2\pi/\omega$ vanish so that α_{31} and α_{32} are simply oscillations around zero, and that they change their signs under time shifts by π/ω . Our reasoning for α_{ij} applies analogously to η_{ij} .

We write down the result of these considerations in the form

$$\begin{aligned} \alpha_{11} &= \tilde{\alpha}(t) & \alpha_{22} &= \tilde{\alpha}(t - \pi/2\omega) \\ \alpha_{12} &= -\tilde{\gamma}(t) & \alpha_{21} &= \tilde{\gamma}(t - \pi/2\omega) \\ \alpha_{31} &= \tilde{\kappa}(t) & \alpha_{32} &= \tilde{\kappa}(t - \pi/2\omega) \\ \eta_{11} &= \tilde{\eta}_t(t) & \eta_{22} &= \tilde{\eta}_t(t - \pi/2\omega) \\ \eta_{12} &= -\tilde{\delta}(t) & \eta_{21} &= \tilde{\delta}(t - \pi/2\omega) \\ \eta_{31} &= \tilde{\lambda}(t) & \eta_{32} &= \tilde{\lambda}(t - \pi/2\omega) \end{aligned} \quad (12)$$

Here $\tilde{\alpha}$, $\tilde{\gamma}$, $\tilde{\eta}_t$ and $\tilde{\delta}$ are in general periodic functions of time with the basic period π/ω , but $\tilde{\kappa}$ and $\tilde{\lambda}$ are periodic functions with period $2\pi/\omega$, which show sign changes under any time shift by π/ω and vanish under averaging over the period $2\pi/\omega$.

From (9) and (12) we conclude

$$\begin{aligned} \overline{\mathcal{E}} &= \tilde{\alpha}(\hat{x} \cdot \overline{\mathbf{B}})\hat{x} + \tilde{\alpha}^\dagger(\hat{y} \cdot \overline{\mathbf{B}})\hat{y} \\ &\quad - \tilde{\gamma}(\hat{y} \cdot \overline{\mathbf{B}})\hat{x} + \tilde{\gamma}^\dagger(\hat{x} \cdot \overline{\mathbf{B}})\hat{y} \\ &\quad - \tilde{\eta}_t(\hat{x} \cdot \overline{\mathbf{J}})\hat{x} - \tilde{\eta}_t^\dagger(\hat{y} \cdot \overline{\mathbf{J}})\hat{y} \\ &\quad + \tilde{\delta}(\hat{y} \cdot \overline{\mathbf{J}})\hat{x} - \tilde{\delta}^\dagger(\hat{x} \cdot \overline{\mathbf{J}})\hat{y} \\ &\quad + [\tilde{\kappa}(\hat{x} \cdot \overline{\mathbf{B}}) + \tilde{\kappa}^\dagger(\hat{y} \cdot \overline{\mathbf{B}}) + \tilde{\lambda}(\hat{x} \cdot \overline{\mathbf{J}}) + \tilde{\lambda}^\dagger(\hat{y} \cdot \overline{\mathbf{J}})] \hat{z}. \end{aligned} \quad (13)$$

Here $\tilde{\alpha}^\dagger$, $\tilde{\gamma}^\dagger$, $\tilde{\eta}_t^\dagger$ and $\tilde{\delta}^\dagger$ differ only by a phase shift of $\pi/2$ from $\tilde{\alpha}$, $\tilde{\gamma}$, $\tilde{\eta}_t$ and $\tilde{\delta}$, respectively, and $\tilde{\kappa}^\dagger$ and $\tilde{\lambda}^\dagger$ by a phase shift of π from $\tilde{\kappa}$ and $\tilde{\lambda}$.

In addition to fields as defined above by averaging over x and y we consider also time-averaged mean fields defined by additional averaging over a time interval of length $2\pi/\omega$ (but we refer to them only if explicitly indicated). When speaking of time averaging in what follows we always refer to this interval. For time-averaged mean fields (13) turns into

$$\overline{\mathcal{E}} = \alpha [\overline{\mathbf{B}} - (\hat{z} \cdot \overline{\mathbf{B}})\hat{z}] + \gamma \hat{z} \times \overline{\mathbf{B}} - \eta_t \overline{\mathbf{J}} - \delta \hat{z} \times \overline{\mathbf{J}}, \quad (14)$$

where α , γ , η_t and δ are time averages of $\tilde{\alpha}$, $\tilde{\gamma}$, $\tilde{\eta}_t$ and $\tilde{\delta}$.²

In the special case of the Roberts flow, i.e. $\epsilon = 0$, the coefficient $\tilde{\alpha}$ is independent of time and so coincides with $\tilde{\alpha}^\dagger$, and this applies analogously to $\tilde{\gamma}$, $\tilde{\eta}_t$, $\tilde{\delta}$, $\tilde{\kappa}$ and $\tilde{\lambda}$. In addition in this case the inversion of \hat{z} in (2) is equivalent to a shift of the flow pattern, e.g., by $\pi/\sqrt{2}k_H$ along $y = x$. Since such a shift does not change averages, $\overline{\mathcal{E}}$ as given by (14) must be even in \hat{z} . Therefore we have then $\gamma = \delta = 0$. Nonzero γ and δ terms in (14) require a break of this

symmetry, that is, a preference of \hat{z} over $-\hat{z}$, and this may occur as a consequence of the aforementioned circular motion of the flow pattern.

We override for a moment our restriction to non-negative values of the frequency ω and admit also negative ones. For $\omega > 0$ the circular motion of the flow pattern defines, together with the z direction, a right-handed screw, and for $\omega < 0$ a left-handed one. We conclude from this fact that inversion of the sign of ω has no other consequences than inversion of the signs of γ and δ .

Second-order approximation

The task of determination of $\overline{\mathcal{E}}$ is now reduced to the determination of the six functions $\tilde{\alpha}$, $\tilde{\gamma}$, $\tilde{\eta}_t$, $\tilde{\delta}$, $\tilde{\kappa}$ and $\tilde{\lambda}$ which occur in (12) and (13). As a first step in that direction we investigate $\overline{\mathcal{E}}$ within the second-order correlation approximation (SOCA). Later we will proceed to a corresponding fourth-order approximation.

SOCA is defined by the neglect of the term with $\mathbf{u} \times \mathbf{b} - \overline{\mathbf{u} \times \mathbf{b}}$ on the right-hand side of equation (8) for \mathbf{b} , which turns so into

$$(\partial_t - \eta \nabla^2)\mathbf{b} = (\overline{\mathbf{B}} \cdot \nabla)\mathbf{u} - (\mathbf{u} \cdot \nabla)\overline{\mathbf{B}}, \quad \nabla \cdot \mathbf{b} = 0. \quad (15)$$

We may solve this equation with \mathbf{u} as given by (2) and (3) analytically and calculate then $\overline{\mathcal{E}}$, see Appendix B. When choosing the form (13) of the result we have

$$\begin{aligned} \tilde{\alpha} &= u_0 R_m \chi^{(2)}(t), \\ \tilde{\eta}_t &= \frac{1}{2} u_0 k_H^{-1} R_m [\chi^{(2)}(t) + \chi^{(2)}(t - \pi/2\omega)], \\ \tilde{\gamma} &= \tilde{\delta} = \tilde{\kappa} = \tilde{\lambda} = 0. \end{aligned} \quad (16)$$

Here we have used the definition

$$R_m = u_0 / \eta k_H, \quad (17)$$

and $\chi^{(2)}$ is given by

$$\chi^{(2)}(t) = \int_0^\infty \text{CC}(\omega t, \omega t - q\tau) e^{-\tau} d\tau \quad (18)$$

where

$$\text{CC}(a, b) = \cos[\epsilon(\cos a - \cos b)] \quad (19)$$

and

$$q = \omega / \eta k_H^2. \quad (20)$$

The parameter q gives, apart from a factor 2π , the ratio of the decay time of a magnetic structure with a length scale $2\pi/k_H$, that is $(2\pi)^2/\eta k_H^2$, and the wobble period $2\pi/\omega$ of the flow pattern. In the case of small q the magnetic field follows the fluid motion immediately, but for large q it does so only with large delay. These two cases are sometimes labelled as “low conductivity limit” and “high conductivity limit”, respectively.

In agreement with the general findings summarized in (12), the function $\chi^{(2)}$ is periodic in time with a basic period π/ω . Whereas $\tilde{\alpha}$ and $\tilde{\alpha}^\dagger$ differ by a phase shift of $\pi/2$, $\tilde{\eta}_t$ and $\tilde{\eta}_t^\dagger$ coincide. $\chi^{(2)}$ satisfies $|\chi^{(2)}| \leq 1$. It must be positive as long as $\epsilon \leq \pi/4$ but may otherwise take negative values, too. If $\epsilon = 0$, or $\epsilon \neq 0$ and $q = 0$ (what corresponds to the low-conductivity limit), $\chi^{(2)}$ is independent of time and equal to unity. In Appendix B some numerically determined values of $\chi^{(2)}$ are given. We note further that

$$\chi^{(2)}(t) = 1 - (\epsilon q)^2 \sin^2 \omega t \quad \text{if } \epsilon q \ll 1 \text{ and } q \ll 1, \quad (21)$$

and

² In view of the signs of α and γ we deviate here from representations as given, e.g., in Rädler et al. (2002a) but follow CHT06.

$$\chi^{(2)}(t) \rightarrow 0 \quad \text{as } q \rightarrow \infty. \quad (22)$$

For time-averaged mean fields we have again (14), now with

$$\alpha = u_0 R_m \chi_0^{(2)}, \quad \eta_t = u_0 k_H^{-1} R_m \chi_0^{(2)}, \quad \gamma = \delta = 0, \quad (23)$$

where $\chi_0^{(2)}$ means the time average of $\chi^{(2)}$ over the period π/ω . We point out that the time average of a function of ωt , say $f(\omega t)$, over an interval of the length π/ω is independent of ω . This is obvious from $(\omega/\pi) \int_0^{\pi/\omega} f(\omega t) dt = (1/\pi) \int_0^\pi f(\varphi) d\varphi$. Hence $\chi_0^{(2)}$ does not explicitly, but only in an indirect way via q , depend on ω .

If $\epsilon = 0$, or $\epsilon \neq 0$ and $q = 0$, we have $\chi_0^{(2)} = 1$. For $\epsilon = 0$ we fall back to the Roberts flow. Indeed, the result (23) with $\chi_0^{(2)} = 1$ agrees with earlier results for this flow; see Appendix A. In view of (23) we note further

$$\chi_0^{(2)} = 1 - \frac{1}{2}(\epsilon q)^2 \quad \text{if } \epsilon q \ll 1 \text{ and } q \ll 1 \quad (24)$$

and

$$\chi_0^{(2)} \rightarrow 0 \quad \text{as } q \rightarrow \infty. \quad (25)$$

The last statement implies $\alpha/u_0 R_m \rightarrow 0$ as $q \rightarrow \infty$.

As we know from general considerations on SOCA (e.g., Krause & Rädler 1980) the range of applicability of SOCA depends on q . For small q a sufficient condition for its validity reads $R_m \ll 1$. For large q such a condition is $R_m/q \ll 1$.

Higher-order approximations

Going now beyond SOCA we start again with Eq. (8) for \mathbf{b} and put

$$\mathbf{b} = \mathbf{b}^{(1)} + \mathbf{b}^{(2)} + \mathbf{b}^{(3)} + \dots \quad (26)$$

with $\mathbf{b}^{(n)}$ being of the order n in \mathbf{u} , and correspondingly

$$\overline{\mathbf{E}} = \overline{\mathbf{E}}^{(2)} + \overline{\mathbf{E}}^{(3)} + \overline{\mathbf{E}}^{(4)} + \dots, \quad \overline{\mathbf{E}}^{(n+1)} = \langle \mathbf{u} \times \mathbf{b}^{(n)} \rangle, \quad n \geq 1. \quad (27)$$

In that sense \mathbf{b} and $\overline{\mathbf{E}}$ in Sect. 2.3 have to be interpreted as $\mathbf{b}^{(1)}$ and $\overline{\mathbf{E}}^{(2)}$, respectively.

From (8) and (26) we obtain (15), now with $\mathbf{b}^{(1)}$ instead of \mathbf{b} , and further

$$\begin{aligned} (\partial_t - \eta \nabla^2) \mathbf{b}^{(n+1)} &= (\mathbf{b}^{(n)} \cdot \nabla) \mathbf{u} - (\mathbf{u} \cdot \nabla) \mathbf{b}^{(n)} \\ &\quad - \nabla \times (\mathbf{u} \times \mathbf{b}^{(n)}), \quad (28) \\ \nabla \cdot \mathbf{b}^{(n+1)} &= 0, \quad n \geq 1. \end{aligned}$$

Using our result for $\mathbf{b}^{(1)}$ and (28) we have calculated $\mathbf{b}^{(2)}$. It turns out that the average of $\mathbf{u} \times \mathbf{b}^{(2)}$ vanishes, that is $\overline{\mathbf{E}}^{(3)} = \mathbf{0}$. In the same way we may calculate $\mathbf{b}^{(3)}$ and $\overline{\mathbf{E}}^{(4)}$. However, these calculations are rather tedious. For the sake of simplicity we have ignored all contributions to $\overline{\mathbf{E}}^{(4)}$ resulting from derivatives of $\overline{\mathbf{B}}$, that is, the terms with $\tilde{\eta}_t$, $\tilde{\delta}$ and $\tilde{\lambda}$ in (13). Some details of the calculations are explained in Appendix C.

Considering the results of all approximations up to the fourth order and referring again to (13) we have now

$$\begin{aligned} \tilde{\alpha} &= u_0 R_m \left[\chi^{(2)}(t) - \frac{1}{2} R_m^2 \chi^{(4\alpha)}(t) \right], \\ \tilde{\gamma} &= \frac{1}{2} u_0 R_m^3 \chi^{(4\gamma)}(t), \quad \tilde{\kappa} = 0. \end{aligned} \quad (29)$$

The functions $\chi^{(4\alpha)}$ and $\chi^{(4\gamma)}$ are given by

$$\begin{aligned} \chi^{(4\alpha)} &= 2 \int_0^\infty \int_0^\infty \int_0^\infty \text{CC}(\omega t, \omega t - q(\tau' + \tau'' + \tau''')) \\ &\quad \text{CS}(\omega t - q\tau', \omega t - q(\tau' + \tau'')) \\ &\quad \exp(-(\tau' + 2\tau'' + \tau''')) d\tau' d\tau'' d\tau''', \end{aligned}$$

$$\begin{aligned} \chi^{(4\gamma)} &= 2 \int_0^\infty \int_0^\infty \int_0^\infty \text{SC}(\omega t, \omega t - q(\tau' + \tau'')) \\ &\quad \text{SS}(\omega t - q\tau', \omega t - q(\tau' + \tau'' + \tau''')) \\ &\quad \exp(-(\tau' + 2\tau'' + \tau''')) d\tau' d\tau'' d\tau''', \end{aligned} \quad (30)$$

with CC as defined by (19) and analogously defined quantities CS, SC and SS,

$$\begin{aligned} \text{CS}(a, b) &= \cos[\epsilon(\sin a - \sin b)], \\ \text{SC}(a, b) &= \sin[\epsilon(\cos a - \cos b)], \\ \text{SS}(a, b) &= \sin[\epsilon(\sin a - \sin b)]. \end{aligned} \quad (31)$$

Note that CC and CS are symmetric but SC and SS antisymmetric in the two arguments.

Like $\chi^{(2)}$ both $\chi^{(4\alpha)}$ and $\chi^{(4\gamma)}$ oscillate with a basic period π/ω . They satisfy $|\chi^{(4\alpha)}| \leq 1$ and $|\chi^{(4\gamma)}| \leq 1$. Further $\chi^{(4\alpha)}$ is positive as long as $|\epsilon| < \pi/4$. In contrast to $\chi^{(4\alpha)}$, however, the time average of $\chi^{(4\gamma)}$ over a period π/ω is equal to zero. Whereas $\chi^{(4\alpha)}$ is even, $\chi^{(4\gamma)}$ is odd in ω . We have further

$$\begin{aligned} \chi^{(4\alpha)} &= 1 - \frac{1}{4}(\epsilon q)^2(1 + 16 \sin^2 \omega t), \\ \chi^{(4\gamma)} &= \frac{5}{2}(\epsilon q)^2 \sin \omega t \cos \omega t, \quad \text{if } \epsilon q \ll 1 \text{ and } q \ll 1, \end{aligned} \quad (32)$$

and

$$\chi^{(4\alpha)}, \chi^{(4\gamma)} \rightarrow 0 \quad \text{as } q \rightarrow \infty. \quad (33)$$

For time-averaged mean fields again relation (14) applies, now with

$$\alpha = u_0 R_m \left[\chi_0^{(2)} - \frac{1}{2} R_m^2 \chi_0^{(4\alpha)} \right], \quad \gamma = 0, \quad (34)$$

where $\chi_0^{(4\alpha)}$ is the time average of $\chi^{(4\alpha)}$. Like $\chi_0^{(2)}$ also $\chi_0^{(4\alpha)}$ does not explicitly depend on ω . Unfortunately, values for η_t and δ are not available. We have

$$\chi_0^{(4\alpha)} = 1 - \frac{9}{4}(\epsilon q)^2, \quad \chi_0^{(4\gamma)} = 0, \quad \text{if } \epsilon q \ll 1 \text{ and } q \ll 1, \quad (35)$$

and

$$\chi_0^{(4\alpha)}, \chi_0^{(4\gamma)} \rightarrow 0 \quad \text{as } q \rightarrow \infty. \quad (36)$$

With (34) we find then

$$\alpha = u_0 R_m \left[1 - \frac{1}{2}(\epsilon q)^2 - \frac{1}{2} R_m^2 (1 - \frac{9}{4}(\epsilon q)^2) \right] \quad \text{if } \epsilon q \ll 1 \text{ and } q \ll 1. \quad (37)$$

Results of higher approximations are very desirable but require heavy efforts. We suspect that in the approximation of sixth order in \mathbf{u} the time averages of $\tilde{\gamma}$ and $\tilde{\delta}$, and so the coefficients γ and δ in (14) no longer vanishes. This presumption is supported by numerical results (see below).

2.4 Mean electromotive force in case (ii)

Modifying the considerations on case (i) properly we may conclude that relation (14), again considered for time-averaged fields, applies for the fluid flow of type (ii) with $\gamma = \delta = 0$. By contrast to case (i) the correlation between velocity components at different times vanishes if the time difference becomes very large.

Modifying also the SOCA calculations described above and in Appendix B correspondingly we find again (23), but with $\chi_0^{(2)}$ being the time average of

$$\chi^{(2)}(t) = \int_0^\infty \cos \left\{ \epsilon [\phi_x(t/\tau_c) - \phi_x(t/\tau_c - q\tau)] \right\} e^{-\tau} d\tau, \quad (38)$$

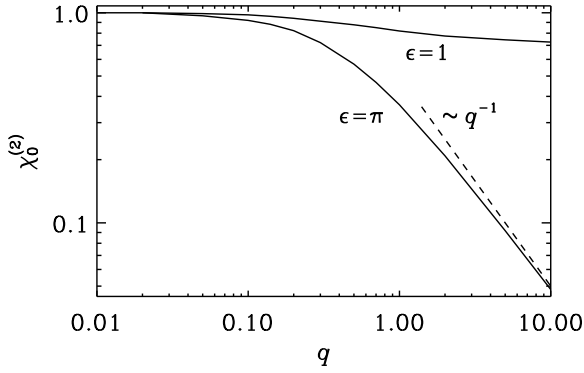


Figure 1. Dependence of $\chi_0^{(2)}$ on q for two different ϵ , calculated numerically on the basis of equation (38). The dashed line shows that $\chi_0^{(2)}$ with $\epsilon = \pi$ behaves like q^{-1} for large q .

where q is now defined by

$$q = (\tau_c \eta k_H^2)^{-1}. \quad (39)$$

We have here again $\chi^{(2)} = 1$ for $q = 0$, and $\chi^{(2)}$ vanishes for $q \rightarrow \infty$. Like $\chi^{(2)}$ also $\chi_0^{(2)}$ depends on ϵ and q but no longer explicitly on τ_c . We have calculated $\chi_0^{(2)}$ on the basis of equation (38) under the assumption that ϕ_x is always constant over time intervals of a given length. Fig. 1 shows dependencies on ϵ and q .

3 TEST-FIELD METHOD

We will determine numerically the elements of the tensors α_{ij} and η_{ij} introduced with (9), but with $1 \leq i, j \leq 2$ only, employing the test-field method of Schrunner et al. (2005, 2007).

We will calculate $\bar{\mathcal{E}} = \overline{\mathbf{u} \times \mathbf{b}}$ from numerical solutions \mathbf{b} of (8), with $\bar{\mathbf{B}}$ replaced by one out of four test fields $\bar{\mathbf{B}}^{pq}$,

$$\begin{aligned} \bar{\mathbf{B}}^{1c} &= B (\cos kz, 0, 0), & \bar{\mathbf{B}}^{2c} &= B (0, \cos kz, 0), \\ \bar{\mathbf{B}}^{1s} &= B (\sin kz, 0, 0), & \bar{\mathbf{B}}^{2s} &= B (0, \sin kz, 0), \end{aligned} \quad (40)$$

where B and k are constants. Repeating this for all test fields, denoting the $\bar{\mathcal{E}}$ that belongs to a given $\bar{\mathbf{B}}^{pq}$ by $\bar{\mathcal{E}}^{pq}$, and using (9) we find

$$\begin{aligned} \bar{\mathcal{E}}_i^{pc}(z) &= B (\alpha_{ip} \cos kz - \eta_{ip}^\dagger k \sin kz), \\ \bar{\mathcal{E}}_i^{ps}(z) &= B (\alpha_{ip} \sin kz + \eta_{ip}^\dagger k \cos kz), \end{aligned} \quad (41)$$

for $1 \leq i, j \leq 2$, where

$$\eta_{ip}^\dagger = \eta_{il} \epsilon_{lp3} = \begin{pmatrix} -\eta_{12} & \eta_{11} \\ -\eta_{22} & \eta_{21} \end{pmatrix}. \quad (42)$$

From this we conclude

$$\begin{aligned} \alpha_{ij} &= B^{-1} [\bar{\mathcal{E}}_i^{jc}(z) \cos kz + \bar{\mathcal{E}}_i^{js}(z) \sin kz], \\ \eta_{ij}^\dagger &= -(kB)^{-1} [\bar{\mathcal{E}}_i^{jc}(z) \sin kz - \bar{\mathcal{E}}_i^{js}(z) \cos kz], \end{aligned} \quad (43)$$

again for $1 \leq i, j \leq 2$.

We point out that, although the $\bar{\mathcal{E}}^{pq}$ depend on z , the α_{ij} and η_{ij} have to be independent of z . We further note that relation (9), on which these considerations are based, can only be justified under the assumption that all higher than first-order spatial derivatives of $\bar{\mathbf{B}}$ are negligible. The derivatives of order n of

our test fields $\bar{\mathbf{B}}^{pq}$ are proportional to k^n . For this reason the results (43) apply in a strict sense only in the limit $k \rightarrow 0$ (cf. Brandenburg, Rädler & Schrunner 2008).

Let us focus here on case (i). After having calculated the α_{ij} and η_{ij} in the way indicated above we may determine the $\tilde{\alpha}$, $\tilde{\gamma}$, $\tilde{\eta}_t$ and $\tilde{\delta}$ according to (12), that is,

$$\begin{aligned} \tilde{\alpha}(t) &= \frac{1}{2} [\alpha_{11}(t) + \alpha_{22}(t + \pi/2\omega)], \\ \tilde{\gamma}(t) &= -\frac{1}{2} [\alpha_{12}(t) - \alpha_{21}(t + \pi/2\omega)], \\ \tilde{\eta}_t(t) &= \frac{1}{2} [\eta_{11}(t) + \eta_{22}(t + \pi/2\omega)], \\ \tilde{\delta}(t) &= -\frac{1}{2} [\eta_{12}(t) - \eta_{21}(t + \pi/2\omega)]. \end{aligned} \quad (44)$$

We are, however, mainly interested in the time-independent coefficients α , γ , η and δ that are relevant for time-averaged mean fields as addressed in (14). They are just time averages of the $\tilde{\alpha}$, $\tilde{\gamma}$, $\tilde{\eta}_t$ and $\tilde{\delta}$, that is

$$\begin{aligned} \alpha &= \frac{1}{2} (\langle \alpha_{11} \rangle + \langle \alpha_{22} \rangle), & \gamma &= -\frac{1}{2} (\langle \alpha_{12} \rangle - \langle \alpha_{21} \rangle) \\ \eta &= \frac{1}{2} (\langle \eta_{11} \rangle + \langle \eta_{22} \rangle), & \delta &= -\frac{1}{2} (\langle \eta_{12} \rangle - \langle \eta_{21} \rangle), \end{aligned} \quad (45)$$

where $\langle \dots \rangle$ means averaging over a time interval of length π/ω . In case (ii) the relations (45) apply with $\langle \dots \rangle$ interpreted as averaging over a sufficiently long time.

4 A GENERALIZATION

So far we have assumed that the mean electromotive force $\bar{\mathcal{E}}$ in a given point is completely determined by $\bar{\mathbf{B}}$ and its first spatial derivatives in this point. If we relax this assumption we may proceed as in Brandenburg, Rädler & Schrunner (2008). In that sense we may replace (9), applied to time-averaged mean fields, by

$$\bar{\mathcal{E}}_i(z) = \int [\hat{\alpha}_{ij}(\zeta) \bar{\mathbf{B}}_j(z - \zeta) - \hat{\eta}_{ij}(\zeta) \bar{\mathbf{J}}_j(z - \zeta)] d\zeta \quad (46)$$

with kernels $\hat{\alpha}_{ij}$ and $\hat{\eta}_{ij}$. When using a Fourier transformation $Q(z) = \int \tilde{Q} \exp(ikz) dz$, this turns into

$$\tilde{\bar{\mathcal{E}}}_i(k) = \tilde{\alpha}_{ij}(k) \tilde{\bar{\mathbf{B}}}_j(k) - \tilde{\eta}_{ij}(k) \tilde{\bar{\mathbf{J}}}_j(k), \quad (47)$$

where

$$\tilde{\alpha}_{ij}(k) = \int \hat{\alpha}_{ij}(\zeta) \cos k\zeta d\zeta, \quad \tilde{\eta}_{ij}(k) = \int \hat{\eta}_{ij}(\zeta) \cos k\zeta d\zeta. \quad (48)$$

In this understanding the relations (41)–(43) apply with α_{ij} and η_{ij} being replaced by $\tilde{\alpha}_{ij}$ and $\tilde{\eta}_{ij}$, which have a well-defined meaning for all k (not only in the limit $k \rightarrow \infty$).

5 RESULTS

5.1 Units and dimensionless parameters

It is appropriate to give $\tilde{\alpha}$ and $\tilde{\gamma}$ as well as α and γ in units of u_0 , and $\tilde{\eta}_t$, $\tilde{\delta}$, η_t and δ in units of u_0/k_H . The remaining dimensionless parts of these coefficients are then, apart from the time dependencies of $\tilde{\alpha}$, $\tilde{\gamma}$, $\tilde{\eta}_t$ and $\tilde{\delta}$, functions of the dimensionless parameters R_m , ϵ and q introduced through (17), (3), and either (20) or (39). Instead of q we may also use the dimensionless quantity $\tilde{\omega}$ defined by

$$\tilde{\omega} = q/R_m. \quad (49)$$

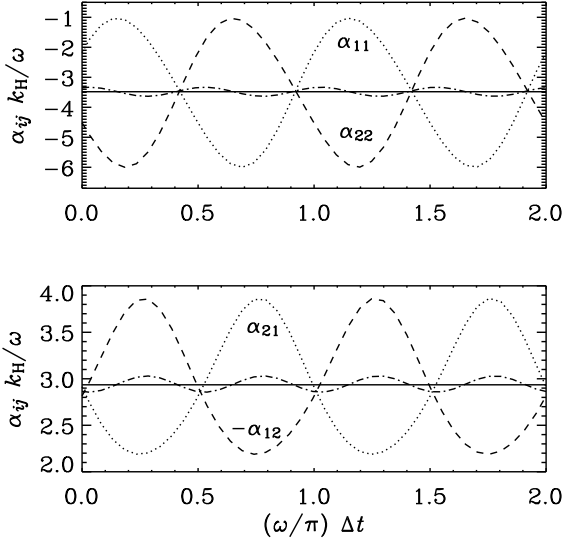


Figure 2. Time dependence of α_{ij} for the parameters used in Fig. 1 of CHT06 which, in our normalization, are $R_m = 78$, $\epsilon = 3/4$, and $\tilde{\omega} = \sqrt{2/3}$. Here, $\Delta t = t - t_0$, where $t_0 = 300/\omega$ is the final time shown in Fig. 1 of CHT06. The dotted lines refer to α_{11} and α_{21} , respectively, the dashed lines to α_{12} and α_{22} , and the dash-dotted lines to $(\alpha_{11} + \alpha_{22})/2$ and $(\alpha_{21} - \alpha_{12})/2$. The straight solid lines give the time averages of the latter quantities, that is, α and γ .

In case (i) we have so $\tilde{\omega} = \omega/u_0 k_H$, which is the ratio of the turnover time $(u_0 k_H/2\pi)^{-1}$ to the wobble period $2\pi/\omega$. In case (ii) applies $\tilde{\omega} = (\tau_c u_0 k_H)^{-1}$, and this is, apart from a factor 2π , the ratio of that turnover time to the time τ_c introduced with the random flow.

5.2 Case (i)

Comparison with CHT06

We show first that our method reproduces results by CHT06. We suppose that our R_m is related to the magnetic Reynolds number, say R_m^{CHT} , used but not explicitly defined there, by $R_m = \sqrt{3/2} R_m^{\text{CHT}}$. While in CHT06 dependencies of the results on R_m and ϵ are considered, no values of q or $\tilde{\omega}$ are given. We suppose that the calculations have actually been carried out with $\tilde{\omega} = \sqrt{2/3}$. Finally we suppose that the unit of α and γ used by CHT06 is ω/k_H .

With a view to Fig. 1 of CHT06 we have carried out calculations with $R_m = \sqrt{3/2} \times 64 \approx 78$, $\epsilon = 3/4$ and $\tilde{\omega} = \sqrt{2/3}$. Our results for the α_{ij} obtained with these parameters and given in this particular case in units of ω/k_H are presented in our Fig. 2. We see in particular that α_{11} and α_{22} vary between -6 and -1 with a period π/ω . As far as α_{11} is concerned this agrees with the result for $\langle \mathbf{u} \times \mathbf{b} \rangle_x$ shown in Fig. 1 of CHT06. Also the initial evolution of α_{11} , which is not shown here, agrees with this figure. Furthermore, in our Fig. 2 the phase shift by $\pi/2$ between α_{11} and α_{22} discussed in Sect. 2.2 is clearly visible. Our results for α_{12} and α_{21} lead to a value of γ , which agrees in modulus but differs in sign from that of CHT06. (To obtain their sign we need to replace ω by $-\omega$.) With the above values of R_m and $\tilde{\omega}$ but $\epsilon = 1$ we find again a sign of γ opposite to that of CHT06.

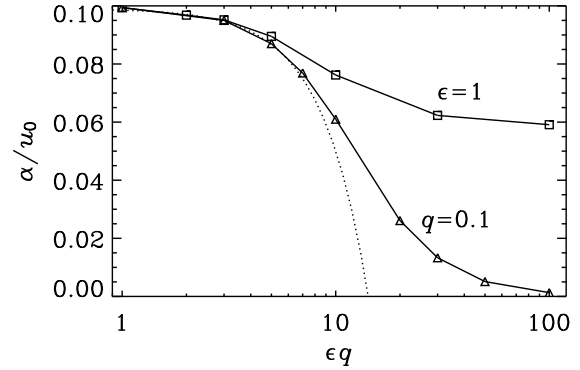


Figure 3. Dependence of α/u_0 on ϵq for $R_m = 0.1$, with $\epsilon = 1$ and with $q = 0.1$. The dotted curve corresponds to (37), which has been derived for $\epsilon q \ll 1$ and $q \ll 1$ only.

Time-averaged mean fields

Switching now to time-averaged mean fields we start with Fig. 3, which shows results for α at $R_m = 0.1$ in dependence on ϵq . They were found with the help of numerical integrations of the test-field version of (8) in its complete form or after reducing it to SOCA. It turned out that SOCA is sufficient for their calculation. Some of these results were also confirmed by evaluating (23) with (18) or (24). As long as ϵq is small, α depends in agreement with (23) and (24) only via this product on ϵ and q . For larger ϵq it depends, however, in a more complex way on ϵ and q . Furthermore, α remains finite if $\epsilon = 1$ and q grows, and it tends to zero if $q = 0.1$ and ϵ grows. Since R_m is small the validity of SOCA is plausible in the case $q = 0.1$. It is however remarkable in that with $\epsilon = 1$, in which q may grow up to 10.

Next, we consider the dependence of α and γ on R_m , in Fig. 4 shown for $\epsilon = 1$ and $\tilde{\omega} = 1$ (i.e. $q = R_m$). For small R_m we expect that SOCA applies and so α/u_0 is linear in R_m but γ vanishes. Indeed α/u_0 shows this linearity up to $R_m \approx 1$. In agreement with the results of CHT06 γ is negative and its modulus remains small for $R_m < 1$. Remarkably the values of α/u_0 calculated from (23) and (24) (dotted line), or (37) (dashed line), which have been derived for $q \ll 1$ and $\epsilon q \ll 1$, deviate for $R_m > 1$ drastically from both the numerically obtained SOCA results (dash-dotted line) and those obtained without any approximation of that kind (solid line). The proportionality of γ/u_0 with R_m^5 confirms the presumption made at the end of Sect. 2.3 that nonzero values of γ occur only in sixth-order and higher approximations with respect to u_0 .

Simple arguments (as given in Sect. 6 below) suggest that α is never negative. However, CHT06 found that not only the moduli but also the signs of both α and γ depend for each given R_m sensitively on ϵ . In our Fig. 5, which applies for $R_m = 100$ and $\tilde{\omega} = \sqrt{2/3}$, both α and γ vary strongly with ϵ , too. The represented results confirm, apart from the sign of γ , the corresponding ones in Fig. 2 of CHT06. Both α and γ change their signs with ϵ . As Fig. 6 shows, in the situation with the same R_m and $\tilde{\omega} = 1$ only γ changes its sign, which indicates a considerable effect of changing $\tilde{\omega}$. In both of the cases considered in Fig. 5 and Fig. 6, α and γ diminish for small as well as large values of ϵ .

In Fig. 7 and Fig. 8 we see that α and γ depend, at least for $R_m = 100$ and $\epsilon = 1$, also sensitively on the parameter $\tilde{\omega}$, or q , that is, on the frequency with which the velocity pattern wobbles.

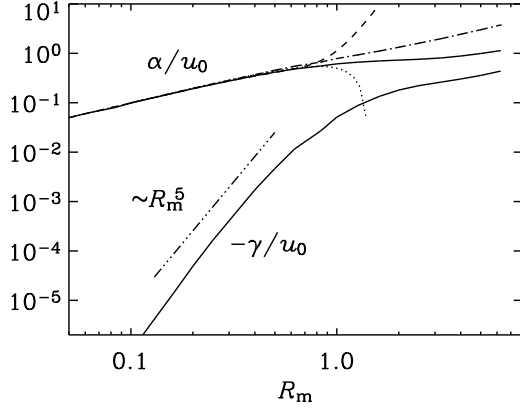


Figure 4. Dependence of α/u_0 and $-\gamma/u_0$ on R_m for $\epsilon = 1$ and $\tilde{\omega} = 1$ (i.e. $q = R_m$). Solid lines show results obtained without any approximation. The dash-dotted line gives α/u_0 as obtained numerically using SOCA. The dotted and the dashed line give results calculated with (23) and (24), or (37), respectively.

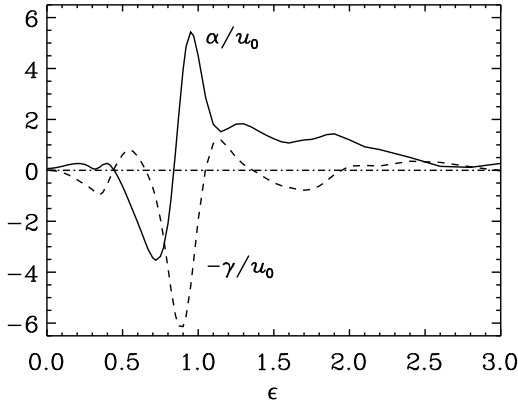


Figure 5. Dependence of α/u_0 and $-\gamma/u_0$ on ϵ for $R_m = 100$, and $\tilde{\omega} = \sqrt{2/3}$ (the value considered by CHT06).

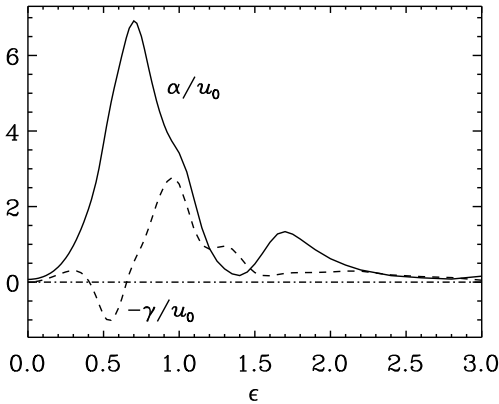


Figure 6. Dependence of α/u_0 and $-\gamma/u_0$ on ϵ for $R_m = 100$, and $\tilde{\omega} = 1$.

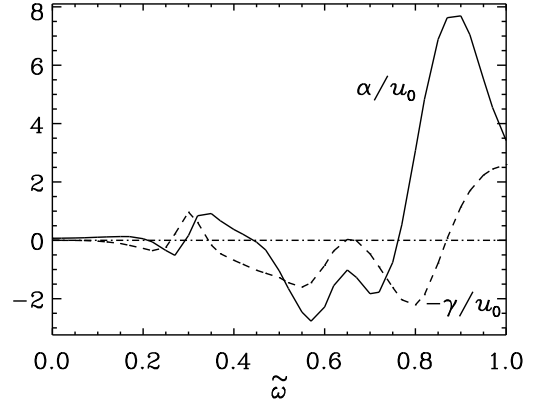


Figure 7. Dependence of α/u_0 and $-\gamma/u_0$ on $\tilde{\omega}$ for $R_m = 100$ and $\epsilon = 1$.

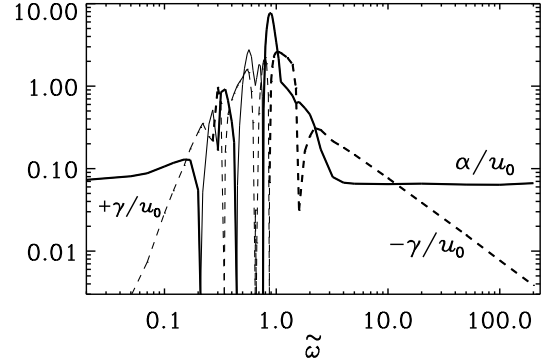


Figure 8. Logarithmic representation of the dependence of $+\alpha/u_0$ (thick solid lines), $-\alpha/u_0$ (thin solid lines), $-\gamma/u_0$ (thick dashed lines), and $+\gamma/u_0$ (thin dashed lines) on $\tilde{\omega}$ for $R_m = 100$ and $\epsilon = 1$. For large values of $\tilde{\omega}$ we have $\alpha/u_0 \approx 0.065$ and $-\gamma/u_0 \approx 0.8/\tilde{\omega}$.

There are, however, simple asymptotic behaviors for small and for large $\tilde{\omega}$, clearly visible for $\tilde{\omega} < 0.1$ and $\tilde{\omega} > 3$. Similar results have been found for $R_m = 10$ and $\epsilon = 1$. In this case, however, α stays positive for all values of $\tilde{\omega}$, and only one sign reversal of γ occurs.

We see from CHT06 that there is a rich dependence of α and γ on R_m for values of $\tilde{\omega}$ and ϵ of order unity. In Fig. 9 we show results for an example with $\tilde{\omega} = 0.5$. Reversals of α are then possible for rather small values of R_m of the order of 10. However, as Fig. 10 shows, such behaviour disappears for $\tilde{\omega} = 10$, in which case α stays always positive and γ always negative. In fact, there is an asymptotic scaling $\alpha/u_0 \sim R_m^{-1/2}$ as $R_m \rightarrow \infty$, and γ approaches a constant finite value as $R_m \rightarrow \infty$.

In a few cases η_t and δ have been determined in addition to α and γ . Results on the dependence of these quantities with $\epsilon = 1$ and $\tilde{\omega} = 0.7$ on R_m are shown in Fig. 11. They have however been calculated with $k = k_H$, not $k \rightarrow 0$, and are therefore at most approximations of the mentioned quantities.

A correct interpretation of these results requires a look on the explanations of Sect. 4 on the non-local connection between $\overline{\mathcal{E}}$, $\overline{\mathcal{B}}$ and $\overline{\mathcal{J}}$ as defined by (46). In that sense the α , γ , η_t and δ in Fig. 11

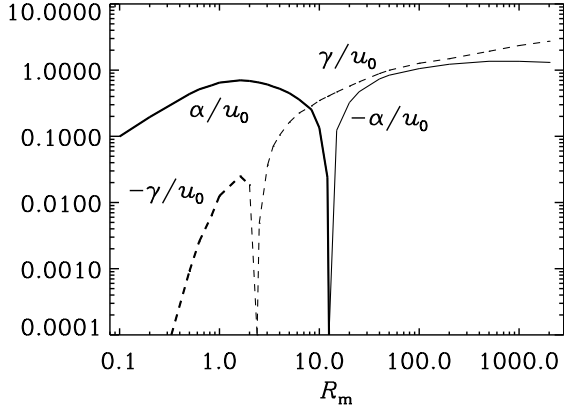


Figure 9. Logarithmic representation of the dependence of α (thick solid line), $-\alpha$ (thin solid line), $-\gamma$ (thick dashed line), and $+\gamma$ (thin dashed line) on R_m for $\tilde{\omega} = 0.5$ for $\epsilon = 1$.

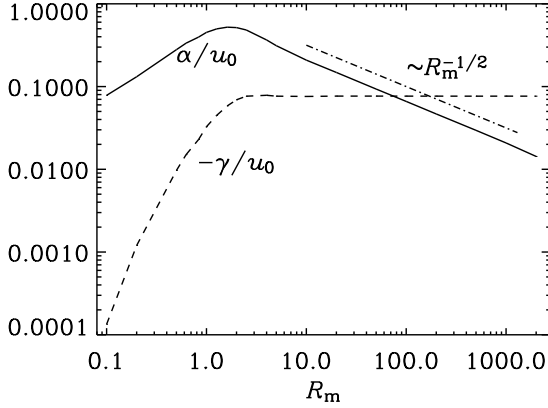


Figure 10. Dependence of α and γ on R_m for $\tilde{\omega} = 10$ for $\epsilon = 1$. Note the asymptotic scaling $\alpha/u_0 \sim R_m^{-1/2}$ (dash-dotted line) and that γ approaches a constant finite value as $R_m \rightarrow \infty$.

may be understood as values of the functions $\tilde{\alpha}(k)$, $\tilde{\gamma}(k)$, $\tilde{\eta}_t(k)$ and $\tilde{\delta}(k)$ at $k = k_H$.

In the following, when writing $\alpha(k)$ or $\eta_t(k)$, for example, we always mean $\tilde{\alpha}(k)$ or $\tilde{\eta}_t(k)$. In an earlier investigation with the Roberts flow under SOCA and with isotropic turbulence independent of SOCA (Brandenburg, Rädler & Schinnerer 2008) it was found that $\alpha(k)$ and $\eta_t(k)$ vary with k in a Lorentzian fashion like $(1+k^2/k_H^2)^{-1}$. However, for the GP flow Courvoisier (2008) found that $\alpha(k)$ at small k is extremely sensitive to the value of R_m .

Fig. 12 shows that $\alpha(k)$ and $\gamma(k)$ for $R_m = 30$, $\tilde{\omega} = 0.5$, and $\epsilon = 1$, approach the values given in Fig. 9 as $k \rightarrow 0$. However, the magnitudes of $\eta_t(k)$ and $\delta(k)$ become rather large as $k \rightarrow 0$. It turns out that α is positive for $k/k_H > 0.4$ and γ becomes smaller with increasing k . Remarkably, $\eta_t(k)$ is negative for $k/k_H < 1$, suggesting that magnetic field generation might be possible via a negative magnetic diffusion instability.

In order to check this possibility we have calculated the linear growth rates

$$\lambda_{\pm}(k) = -[\eta + \eta_t(k)]k^2 \pm \alpha(k)k. \quad (50)$$

Fig. 13 shows that λ_{\pm} is almost entirely given by $\pm\alpha(k)k$. A neg-

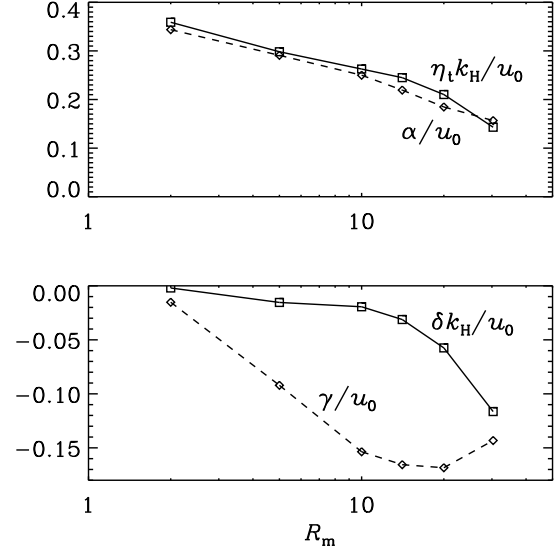


Figure 11. Dependence of α and γ (dashed lines) as well as η_t and δ (solid lines) on R_m , for $\tilde{\omega} = 0.7$, $\epsilon = 1$, and $k = k_H$.

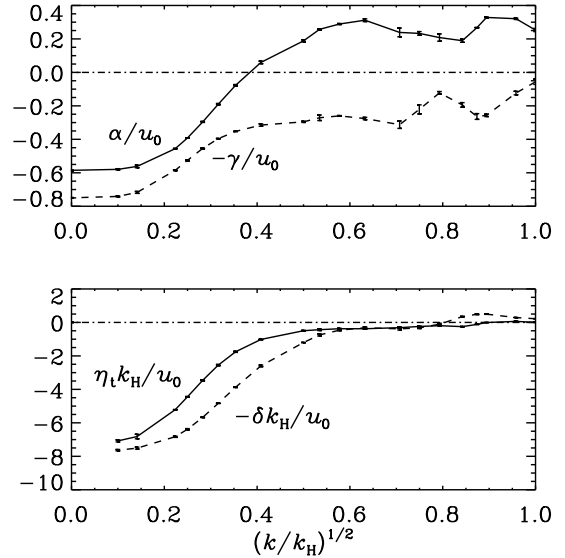


Figure 12. Functions $\alpha(k)$, $\gamma(k)$, $\eta_t(k)$, and $\delta(k)$ for $R_m = 30$, $\tilde{\omega} = 0.5$, and $\epsilon = 1$.

ative diffusivity instability does not occur. It is important to realize that most of the small wavenumber modes, especially those with negative values of η_t , would never be realized. This is because in a system of given size, only the corresponding harmonics will have a chance to be excited, and of those only the ones with the largest growth rates will dominate. We should point out that the detailed variations of λ_+ shown in Fig. 13 may not be accurate. In fact, this figure shows a maximum at $k/k_H \approx 0.75$, but direct simulations suggest that the fastest growth occurs for $k/k_H \approx 0.5$ with a growth rate of $\lambda \approx 0.23 u_{\text{rms}} k_f$. Nevertheless, this value is still compatible with Fig. 13.

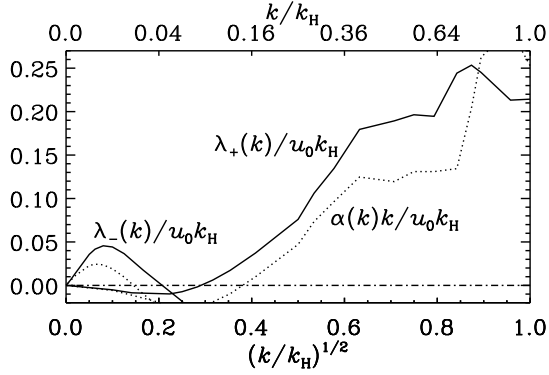


Figure 13. Dependence of λ_{\pm} on k for $R_m = 30$, $\tilde{\omega} = 0.5$, and $\epsilon = 1$. The dotted lines give $\pm\alpha k$ for comparison.

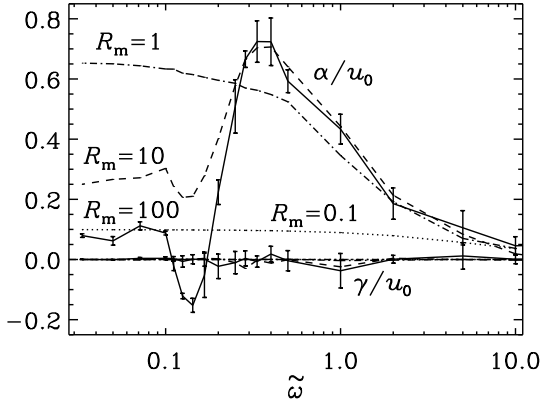


Figure 14. Dependence of α and γ on $\tilde{\omega}$ for the flow with random time dependence (case ii), with $R_m = 100$ (solid lines), $R_m = 10$ (dashed lines), $R_m = 1$ (dash-dotted lines), and $R_m = 0.1$ (dotted lines), and with $\epsilon = \pi$. The error bars are similar in all cases, but are only shown for $R_m = 100$.

5.3 Case (ii)

In case (ii) we have calculated α and γ under the assumptions on ϕ_x and ϕ_y introduced in Sect. 2.4. Fig. 14 shows results for R_m ranging from 0.1 to 100 and $\epsilon = \pi$ as functions of $\tilde{\omega}$. In the limit of small $\tilde{\omega}$ the flow can be considered as stationary, that is, as a Roberts flow. Indeed in this limit the values of α agree well with those obtained for the Roberts flow (e.g., Rädler et al. (2002a), see also Appendix A). For large values of $\tilde{\omega}$ the values of α vanish for all R_m . For not too small $\tilde{\omega}$ and R_m there is no longer a noticeable variation of α with R_m , and α reaches a maximum at $\tilde{\omega} \approx 0.3$. In the range $0.3 \leq \tilde{\omega} \leq 1$ continuous flow renewal removes the tendency for α to diminish with growing R_m . For $\tilde{\omega} \leq 0.2$ the value of α remains strongly dependent on R_m and can still change sign. We have also calculated α with $\epsilon = 1$ and $R_m = 100$ as a function of $\tilde{\omega}$ and found a qualitatively similar behavior as for $\epsilon = \pi$. In this case it remains positive and is up to 50% smaller than for $\epsilon = \pi$ when $\tilde{\omega} < 1$ and somewhat larger when $\tilde{\omega} > 1$. In all cases we found, as expected, $\gamma = 0$ within error margins.

6 DISCUSSION

Our results for the flow of type (i) confirm the finding of CHT06 that both the α and γ coefficients depend sensitively on R_m and also on ϵ , and that even the signs of these coefficients may vary with these parameters. We have to add that α and γ depend also on $\tilde{\omega}$, or $q = \tilde{\omega} R_m$, that is, on parameters connected with the frequency of the wobbling motion, which CHT06 fixed in a special way without commenting on it, and that they show similar variations with these parameters. We found however rather regular behaviors of α and γ for small and for large values of ϵ and $\tilde{\omega}$.

It is sometimes considered as a rule that the sign of α is opposite to that the mean helicity of the fluid flow and its modulus is proportional to that of the mean helicity. There is however no general reason for that kind of relation between α and the kinetic helicity. We see only two limiting cases which allow simple statements on the sign of α .

Firstly, in the framework of SOCA applied to homogeneous turbulence and comparable flows it turns out that the sign of α in the limit $q \rightarrow 0$ is always opposite to that of $\tilde{\psi} \cdot (\nabla \times \tilde{\psi})$, where $\mathbf{u} = \nabla \times \tilde{\psi}$, $\nabla \cdot \tilde{\psi} = 0$; see, e.g., Krause & Rädler (1980); Rädler & Brandenburg (2003). For both types of flows, (i) and (ii), we have $\tilde{\psi} = (\tilde{\psi}_x, -\tilde{\psi}_y, \tilde{\psi}_z)$, where $\tilde{\psi}_x = -k_H(\partial\psi/\partial x + \partial\psi/\partial y)$ and therefore $\tilde{\psi} \cdot (\nabla \times \tilde{\psi}) = -2u_0^2/k_H$. This implies that α is positive. Indeed, only positive α have been observed for small q , even beyond SOCA.

Secondly it was found in SOCA under the same conditions, but in the limit $q \rightarrow \infty$, that the sign of α for a flow with finite correlation time is opposite to that of $\int_0^\infty \mathbf{u}(\mathbf{x}, t) \cdot (\nabla \times \mathbf{u}(\mathbf{x}, t - \tau)) d\tau$; see, e.g., again Krause & Rädler (1980). A relation of that kind between α and this integral can indeed be formally derived from the general relation (29) of Rädler & Rheinhardt (2007) and applied to our specific situation. In case (i) the correlation time is however infinite and this integral does not converge. Although we know that $\mathbf{u} \cdot (\nabla \times \mathbf{u}) = -2u_0^2/k_H$ we do not see how reliable conclusions could be drawn concerning the sign of α in the limit $q \rightarrow \infty$. In case (ii) the integral is positive, and indeed only positive α have been observed.

Beyond the low and high conductivity limits, that is, for not too small or not too large values of q , even SOCA offers no simple general statements on the sign of α . In general α may take both positive and negative values.

For studying α and η_t with very simple flows it seems appropriate to consider flows of type (ii) rather than of type (i). In case (i) the results are influenced by the aforementioned circular motion of the flow pattern. As long as only α and η_t should be discussed there is hardly a reason to introduce such a motion. We see no natural interpretation of it and so no interpretation of the so caused γ and δ effects.

Recently Tilgner (2008) pointed out that a time-dependent flow of a conducting fluid can act as a dynamo even when steady flows which coincide with it at any particular time cannot. He demonstrated this with a Roberts flow modified by a drift of its pattern so that the velocity \mathbf{u} satisfies relations like (2) and (3) with $\varphi_x = -k_H v_d t$ and $\varphi_y = 0$, where v_d is constant the drift velocity. Even if the intensity of the flow is too weak so that in the case $v_d = 0$ no growing solutions of the induction equation with a given period in the z direction exist, such solutions may occur in an interval of some finite v_d . Although this flow considered by Tilgner is in a sense simpler than the flows in our paper, it shows no longer the symmetries with respect to the z axis which we have

utilized. As a consequence the relation between the mean electromotive force $\overline{\mathcal{E}}$ and the mean magnetic field $\overline{\mathbf{B}}$ is more complex. In particular (13) and (14) no longer apply. Nevertheless the question arises whether the effect of the time-dependence of flows observed by Tilgner occurs also in the examples investigated here. In case (i) the parameter ω could play the role of v_d . The fact that the magnitude of α is larger for some finite $\tilde{\omega}$ than for $\tilde{\omega} = 0$, which can be seen in Figs 7 and 8, points in this direction.

One of the original motivations for looking at the GP flow was the fact that it is time-dependent and in that sense closer to turbulent flows than time-independent flows. However, as we have shown here, the dynamo properties of the GP flow cannot be compared in a meaningful way with analytic theories or with simulations that apply to isotropic turbulence. Nevertheless, as shown in this paper, an analytic theory for the α effect and other turbulent transport coefficients can be derived that matches numerical results in limiting cases.

Astrophysical flows can often neither be described by isotropic turbulence nor by wobbling two-dimensional flow patterns, but they are likely to contain aspects of both extremes. However, the present work highlights another aspect that may be of more general significance and concerns the turbulent transport properties in the presence of high-frequency time variability. This is not just a peripheral aspect of turbulence, but it is an additional property whose effects need to be understood more thoroughly. The situation is reminiscent of the modifications of mixing length theory in the presence of stellar pulsations (see, e.g., Gough 1977). In dynamo theory the issue of high-frequency time variability has only recently been addressed. One example concerns the nonlinear α effect where its time dependence has a striking effect on the behaviour of the mean field. In that example the temporal behaviour of the forcing function (delta-correlated or steady) determines the nonlinear asymptotic scaling behavior of the quenching function $\alpha(\overline{\mathbf{B}})$ at low R_m . The early results of Moffatt (1972) and Rüdiger (1974) suggested a $|\alpha| \sim |\overline{\mathbf{B}}|^{-3}$ behavior, but in more recent years Field et al. (1999) and Rogachevskii & Kleeorin (2000) found instead a $|\alpha| \sim |\overline{\mathbf{B}}|^{-2}$ behavior, which seemed in conflict with the earlier results. However, the work of Sur et al. (2007) now shows that this is not just an artifact related to different approximations, for example, but it depends on whether or not the flow is time-dependent. They found that the $|\alpha| \sim |\overline{\mathbf{B}}|^{-3}$ behavior is reproduced if the flow is steady, while the $|\alpha| \sim |\overline{\mathbf{B}}|^{-2}$ behavior is obtained in the time-dependent case using a forcing function that is δ -correlated in time. Again, it is not clear which types of flows are more astrophysically relevant, but it is now clear that the detailed time-dependence of the turbulent flows can affect its transport properties in rather unexpected ways.

ACKNOWLEDGMENTS

We acknowledge Nordita and the Kavli Institute for Theoretical Physics for providing a stimulating atmosphere during their programs on dynamo theory in 2008. This research was supported in part by the National Science Foundation under grant PHY05-51164.

REFERENCES

Brandenburg A., Rädler K.-H., Rheinhardt M., Käpylä P. J. 2008, *ApJ*, 676, 740

- Brandenburg A., Rädler K.-H., Schrunner M. 2008, *A&A*, 482, 739
- Courvoisier A. 2008, *Geophys. Astrophys. Fluid Dyn.*, 102, 217
- Courvoisier A., Hughes D. W., Tobias S. M. 2006, *Phys. Rev. Lett.*, 96, 034503
- Field G. B., Blackman E. G., Chou H. 1999, *ApJ*, 513, 638
- Galloway, D. J., Proctor, M. R. E. 1992, *Nat*, 356, 691
- Gough, D. O. 1977, *ApJ*, 214, 196
- Krause F., Rädler K.-H. 1980, *Mean-field magnetohydrodynamics and dynamo theory* (Pergamon Press, Oxford)
- Moffatt H. K. 1972, *J. Fluid Mech.*, 53, 385
- Moffatt H. K. 1978, *Magnetic field generation in electrically conducting fluids* (Cambridge University Press, Cambridge)
- Parker E. N. 1979, *Cosmical magnetic fields* (Clarendon Press, Oxford)
- Rädler K.-H., Rheinhardt M., Apstein E., Fuchs H. 2002a, *Magnetohydrodynamics*, 38, 41.
- Rädler K.-H., Rheinhardt M., Apstein E., Fuchs H. 2002b, *Nonlinear Processes Geophys.*, 9, 171.
- Rädler K.-H., Brandenburg A. 2003, *Phys. Rev. E*, 67, 026401
- Rädler K.-H., Rheinhardt M. 2007, *Geophys. Astrophys. Fluid Dyn.*, 101, 117
- Roberts G. O. 1972, *Phil. Trans. Roy. Soc. London A*, 271, 411
- Rogachevskii I., Kleeorin N. 2000, *Phys. Rev. E*, 61, 5202
- Rüdiger G. 1974, *AN*, 295, 275
- Schrinner M., Rädler K.-H., Schmitt D., Rheinhardt M., Christensen U. 2005, *AN*, 326, 245
- Schrinner M., Rädler K.-H., Schmitt D., Rheinhardt M., Christensen U. 2007, *Geophys. Astrophys. Fluid Dyn.*, 101, 81
- Soward A. 1987, *J. Fluid Mech.*, 180, 267
- Soward A. 1989, *Geophys. Astrophys. Fluid Dyn.*, 49, 3
- Sur S., Subramanian K., Brandenburg A. 2007, *MNRAS*, 376, 1238
- Sur S., Brandenburg A., Subramanian K. 2008, *MNRAS*, 385, L15
- Tilgner A. 2008, *Phys. Rev. Lett.*, 100, 128501

APPENDIX A: ROBERTS FLOW

In the special case $\epsilon = 0$ the Galloway–Proctor flow, defined by (2) and (3), turns into the Roberts flow. Our SOCA results for this special case agree with results for the Roberts flow reported in Brandenburg et al. (2008) and in Rädler et al. (2002a), referred to as BRS08 and R02a, respectively.

In BRS08 instead of our coordinate system (x, y, z) another one, say (x', y', z) , is used, which is obtained by a 45° rotation of our system about the z axis, that is,

$$x = \frac{1}{\sqrt{2}}(x' - y'), \quad y = \frac{1}{\sqrt{2}}(x' + y'). \quad (\text{A1})$$

In the case $\epsilon = 0$, to which we restrict ourselves here, (3) turns under this transformation into

$$\psi = \frac{2u_0}{k_H} \cos(k_H x' / \sqrt{2}) \cos(k_H y' / \sqrt{2}). \quad (\text{A2})$$

Together with (2) we find so, referring to the system (x', y', z) ,

$$\mathbf{u} = \sqrt{2}u_0 \begin{pmatrix} -\cos(k_H x' / \sqrt{2}) \sin(k_H y' / \sqrt{2}) \\ +\sin(k_H x' / \sqrt{2}) \cos(k_H y' / \sqrt{2}) \\ -\sqrt{2} \cos(k_H x' / \sqrt{2}) \cos(k_H y' / \sqrt{2}) \end{pmatrix}. \quad (\text{A3})$$

Comparing this first with (BRS08 25) and ignoring the opposite sign of u_z we find

$$u_0^{\text{BRS}} = \sqrt{2} u_0, \quad k_0 = k_f/\sqrt{2} = k_H/\sqrt{2}. \quad (\text{A4})$$

The only consequence of inverting the sign of u_z is a sign change of α . Taking then the SOCA results (BRS08 30) for α and η_t , with u_0^{BRS} in place of u_0 and completed by (BRS08 29), considering (A4) and the remark on the sign of α we can easily reproduce our results (23).

This applies analogously to R02a if, in addition to the transformation (A1), x' is replaced by $x' - \pi/\sqrt{2}k_H$ and y' by $y' + \pi/\sqrt{2}k_H$. Comparing the corresponding modification of (A3) with (R02a 15) we find

$$u_\perp = (2\sqrt{2}/\pi)u_0, \quad u_\parallel = (8/\pi^2)u_0, \quad a = \sqrt{2}\pi/k_H. \quad (\text{A5})$$

When using (R02a 19) we obtain our result (23) for α . With (R02a 38) and $\eta_t = \beta_\perp + \beta_3$ we may also reproduce our result (23) for η_t .

Going beyond SOCA we note that according to (BRS08 25), or also according to (R02a 20),

$$\alpha = u_0 R_m \phi(2R_m) \quad (\text{A6})$$

with a function ϕ satisfying $\phi(0) = 1$ and vanishing like $R_m^{-3/2}$ with growing R_m . It has been calculated numerically and is plotted, e.g., in R02a.

APPENDIX B: SECOND-ORDER CALCULATIONS

For the calculation of the α_{ij} and η_{ij} with $1 \leq i, j \leq 2$ under SOCA we start with (15). Introducing there $\mathbf{b} = \text{Re}(\hat{\mathbf{b}} \exp ikz)$ and $\bar{\mathbf{B}} = \text{Re}(\hat{\mathbf{B}} \exp ikz)$ we obtain

$$[\partial_t - \eta(\nabla^2 - k^2)] \hat{\mathbf{b}} = (\hat{\mathbf{B}} \cdot \nabla) \mathbf{u} - ik u_z \hat{\mathbf{B}}. \quad (\text{B1})$$

For our purposes it is useful to represent \mathbf{u} in the form

$$\begin{aligned} u_x &= -u_0 [\cos(k_H y) \text{ss}(t) + \sin(k_H y) \text{cs}(t)], \\ u_y &= u_0 [\cos(k_H x) \text{sc}(t) + \sin(k_H x) \text{cc}(t)], \\ u_z &= -u_0 [\cos(k_H x) \text{cc}(t) - \sin(k_H x) \text{sc}(t) \\ &\quad + \cos(k_H y) \text{cs}(t) - \sin(k_H y) \text{ss}(t)], \end{aligned} \quad (\text{B2})$$

where

$$\text{ss}(t) = \sin(\epsilon \sin \omega t), \quad \text{cs}(t) = \cos(\epsilon \sin \omega t), \quad \text{etc.} \quad (\text{B3})$$

Then the right-hand side of (B1), say $\hat{\mathbf{R}}$, takes then the form

$$\begin{aligned} \hat{\mathbf{R}} &= \hat{\mathbf{R}}^{cx} \cos k_H x + \hat{\mathbf{R}}^{sx} \sin k_H x \\ &\quad + \hat{\mathbf{R}}^{cy} \cos k_H y + \hat{\mathbf{R}}^{sy} \sin k_H y \end{aligned} \quad (\text{B4})$$

with $\hat{\mathbf{R}}^{cx}, \hat{\mathbf{R}}^{sx}, \dots$ depending on time.

Clearly, (B1) poses an initial value problem. As initial time t_0 we take $t_0 \rightarrow -\infty$. Then the solution $\hat{\mathbf{b}}$ of (B1) is completely determined by its right-hand side, $\hat{\mathbf{R}}$, and has again the form of $\hat{\mathbf{R}}$ as given by (B4). Since $\nabla^2 \hat{\mathbf{b}} = -k_H^2 \hat{\mathbf{b}}$ we have

$$\hat{\mathbf{b}}(t) = \int_0^\infty \hat{\mathbf{R}}(t-t') \exp[-\eta(k_H^2 + k^2)t'] dt'. \quad (\text{B5})$$

After determining the $\hat{\mathbf{R}}^{cx}, \hat{\mathbf{R}}^{sx}, \dots$ we find for the analogously defined $\hat{\mathbf{b}}^{cx}, \hat{\mathbf{b}}^{sx}, \dots$

$$\begin{aligned} \hat{b}_x^{cx} &= iu_0 k \hat{B}_x \Gamma(\text{cc}), \quad \hat{b}_x^{sx} = -iu_0 k \hat{B}_x \Gamma(\text{sc}), \\ \hat{b}_x^{cy} &= -u_0 (k_H \hat{B}_y - ik \hat{B}_x) \Gamma(\text{cs}), \\ \hat{b}_x^{sy} &= u_0 (k_H \hat{B}_y - ik \hat{B}_x) \Gamma(\text{ss}), \\ \hat{b}_y^{cx} &= u_0 (k_H \hat{B}_y + ik \hat{B}_x) \Gamma(\text{cc}), \end{aligned}$$

Table B1. Some values of $\chi^{(2)}$ defined in equation (18).

$\frac{\omega t}{\pi/8}$	$\epsilon = 0.1$	$\epsilon = 0.1$	$\epsilon = 1$	$\epsilon = 1$	$\epsilon = 10$	$\epsilon = 10$
	$q = 1$	$q = 10$	$q = 1$	$q = 10$	$q = 1$	$q = 10$
0	0.9970	0.9926	0.7558	0.4204	0.3017	0.2073
1	0.9982	0.9936	0.8521	0.4882	0.5246	0.2667
2	0.9990	0.9954	0.9123	0.6165	-0.1882	-0.1816
3	0.9989	0.9971	0.8963	0.7341	0.1567	0.1912
4	0.9980	0.9975	0.8115	0.7658	-0.1558	-0.2448
5	0.9968	0.9965	0.7121	0.6889	0.1196	0.1881
6	0.9960	0.9947	0.6586	0.5550	-0.0363	-0.1637
7	0.9961	0.9931	0.6775	0.4465	0.1317	0.2189
8	0.9970	0.9926	0.7558	0.4204	0.3017	0.2073

$$\hat{b}_y^{sx} = -u_0 (k_H \hat{B}_y + ik \hat{B}_x) \Gamma(\text{sc}), \quad (\text{B6})$$

$$\hat{b}_y^{cy} = iu_0 k \hat{B}_y \Gamma(\text{cs}), \quad \hat{b}_y^{sy} = -iu_0 k \hat{B}_y \Gamma(\text{ss}),$$

$$\hat{b}_z^{cx} = u_0 k_H \hat{B}_x \Gamma(\text{sc}), \quad \hat{b}_z^{sx} = u_0 k_H \hat{B}_x \Gamma(\text{cc}),$$

$$\hat{b}_z^{cy} = u_0 k_H \hat{B}_y \Gamma(\text{ss}), \quad \hat{b}_z^{sy} = u_0 k_H \hat{B}_y \Gamma(\text{cs}),$$

where

$$\Gamma(f) = \int_0^\infty f(t-t') \exp[-\eta(k_H^2 + k^2)t'] dt' \quad (\text{B7})$$

with any function $f = f(t)$. Of course, Γ depends in general on time. In view of (B6) we note that, since $\bar{\mathbf{B}} = \text{Re}(\hat{\mathbf{B}} \exp ikz)$, we have also $\bar{\mathbf{J}} = \text{Re}(\hat{\mathbf{J}} \exp ikz)$ and therefore $ik \hat{B}_x = \hat{J}_y$ and $ik \hat{B}_y = -\hat{J}_x$.

Calculating then $\bar{\mathcal{E}}$ we find

$$\begin{aligned} \bar{\mathcal{E}}_x &= \overline{u_y b_z} - \overline{u_z b_y} = u_0 R_m a_{xx} \bar{B}_x - u_0 R_m b_{xx} \bar{J}_x \\ \bar{\mathcal{E}}_y &= \overline{u_z b_x} - \overline{u_x b_z} = u_0 R_m a_{yy} \bar{B}_y - u_0 R_m b_{yy} \bar{J}_y \\ \bar{\mathcal{E}}_z &= \overline{u_x b_y} - \overline{u_y b_x} = 0. \end{aligned} \quad (\text{B8})$$

where a_{xx}, a_{yy}, b_{xx} and b_{yy} are in general periodic functions of time, which are defined by

$$\begin{aligned} a_{xx} &= \eta k_H^2 [\text{cc}\Gamma(\text{cc}) + \text{sc}\Gamma(\text{sc})], \\ a_{yy} &= \eta k_H^2 [\text{cs}\Gamma(\text{cs}) + \text{ss}\Gamma(\text{ss})], \\ b_{xx} &= b_{yy} = \frac{1}{2} (a_{xx} + a_{yy}). \end{aligned} \quad (\text{B9})$$

The combination of trigonometric functions on the right-hand side of the relation for a_{xx} can easily be expressed by the function CC defined by (19). The same applies to a_{yy} and the function CS defined in (31).

The result given by (B8) and (B9) is valid for arbitrary k . This applies of course also if it is written in the alternative form with CC and CS. In that sense it is of some interest in view of the nonlocal connection between $\bar{\mathcal{E}}$ and $\bar{\mathbf{B}}$ studied in the paper by Brandenburg, Rädler & Schrunner (2008). In the main part of the present paper we consider however the limit $k \rightarrow 0$ only. In this limit (B7) applies with $k = 0$. Then (B8) and (B9) agree just with (16) and (19).

APPENDIX C: HIGHER-ORDER CALCULATIONS

For the sake of simplicity we assume now, beyond SOCA, that $\bar{\mathbf{B}}$ is a uniform field, that is, has no spatial derivatives. Then $\bar{\mathbf{u}} \times \bar{\mathbf{b}}$ is independent of space coordinates and (28) turns into

$$(\partial_t - \eta \nabla^2) \mathbf{b}^{(n+1)} = (\mathbf{b}^{(n)} \cdot \nabla) \mathbf{u} - (\mathbf{u} \cdot \nabla) \mathbf{b}^{(n)}, \quad n \geq 1. \quad (\text{C1})$$

We may apply some modification of the procedure used in Appendix B for solving the equation (B1) for $\hat{\mathbf{b}}$ to the equations (C1) for $\mathbf{b}^{(2)}$ and $\mathbf{b}^{(3)}$.

The right-hand side of the equation for $\mathbf{b}^{(2)}$, say $\mathbf{R}^{(2)}$, is a linear combination of products $\varphi(x)\varphi(y)$, where $\varphi(x)$ stands for $\cos k_H x$ or $\sin k_H x$, and $\varphi(y)$ for $\cos k_H y$ or $\sin k_H y$. Clearly $\mathbf{b}^{(2)}$ has the same form as $\mathbf{R}^{(2)}$ and satisfies $\nabla^2 \mathbf{b}^{(2)} = -2k_H^2 \mathbf{b}^{(2)}$. Therefore (B5) applies after replacing $\hat{\mathbf{b}}$ and $\hat{\mathbf{R}}$ by $\mathbf{b}^{(2)}$ and $\mathbf{R}^{(2)}$, respectively, k_H^2 by $2k_H^2$, and putting $k = 0$. As a consequence of the described structure of $\mathbf{b}^{(2)}$ we have $\mathbf{u} \times \mathbf{b}^{(2)} = \mathbf{0}$.

The right-hand side of the equation for $\mathbf{b}^{(3)}$, which we call $\mathbf{R}^{(3)}$, is a linear combination of products $\varphi_1(x)\varphi_2(x)\varphi(y)$ or $\varphi(x)\varphi_1(y)\varphi_2(y)$, where the indices 1 and 2 may refer to the same function or to different functions, e.g., $\varphi_1(x) = \varphi_2(x) = \cos k_H x$, or $\varphi_1(x) = \cos k_H x$ and $\varphi_2(x) = \sin k_H x$. In the first case we utilize $\cos^2 k_H x = \frac{1}{2}(1 + \cos 2k_H x)$ and split, e.g., $\cos^2 k_H x \sin k_H y$ into the two parts $\frac{1}{2} \sin k_H y$ and $\frac{1}{2} \cos 2k_H x \sin k_H y$. In this way we may split $\mathbf{R}^{(3)}$ into two parts, $\mathbf{R}^{(3a)}$ and $\mathbf{R}^{(3b)}$, where $\mathbf{R}^{(3a)}$ contains only contributions $\varphi_1(x)\varphi_2(x)\varphi(y)$ and $\varphi(x)\varphi_1(y)\varphi_2(y)$ with three different factors, and contributions of the types $\varphi(x)\varphi(2y)$ and $\varphi(2x)\varphi(y)$, and $\mathbf{R}^{(3b)}$ only contributions of the types $\varphi(x)$ and $\varphi(y)$. There are two corresponding parts of $\mathbf{b}^{(3)}$, that is $\mathbf{b}^{(3a)}$ and $\mathbf{b}^{(3b)}$, which satisfy $\nabla^2 \mathbf{b}^{(3a)} = -5k_H^2 \mathbf{b}^{(3a)}$ and $\nabla^2 \mathbf{b}^{(3b)} = -k_H^2 \mathbf{b}^{(3b)}$ and equations of type of (B5). The structure of $\mathbf{b}^{(3a)}$ implies $\mathbf{u} \times \mathbf{b}^{(3a)} = \mathbf{0}$. Only $\mathbf{b}^{(3b)}$, for which (B5) applies with $\hat{\mathbf{b}}$ and $\hat{\mathbf{R}}$ replaced by $\mathbf{b}^{(3b)}$ and $\mathbf{R}^{(3b)}$, respectively, and $k = 0$, contributes to $\mathbf{u} \times \mathbf{b}^{(3b)}$.

Detailed calculations along these lines deliver us

$$\begin{aligned} \overline{\mathcal{E}}_x^{(4)} &= \overline{u_y b_z^{(3)}} - \overline{u_z b_y^{(3)}} = u_0 R_m^3 (a_{xx} \overline{B}_x + a_{xy} \overline{B}_y) \\ \overline{\mathcal{E}}_y^{(4)} &= \overline{u_z b_x^{(3)}} - \overline{u_x b_z^{(3)}} = u_0 R_m^3 (a_{yx} \overline{B}_x + a_{yy} \overline{B}_y) \\ \overline{\mathcal{E}}_z^{(4)} &= \overline{u_x b_y^{(3)}} - \overline{u_y b_x^{(3)}} = 0. \end{aligned} \quad (\text{C2})$$

with

$$\begin{aligned} a_{xx} &= -(\eta k_H^2)^3 \{ \text{sc}[\Gamma(\text{ss}, \text{ss}, \text{cc}) + \Gamma(\text{cs}, \text{cs}, \text{sc})] \\ &\quad + \text{cc}[\Gamma(\text{ss}, \text{ss}, \text{cc}) + \Gamma(\text{cs}, \text{cs}, \text{cc})] \} \\ a_{xy} &= -(\eta k_H^2)^3 \{ \text{sc}[\Gamma(\text{ss}, \text{cc}, \text{cs}) - \Gamma(\text{cs}, \text{cc}, \text{ss})] \\ &\quad - \text{cc}[\Gamma(\text{ss}, \text{sc}, \text{cs}) - \Gamma(\text{cs}, \text{sc}, \text{ss})] \} \\ a_{yx} &= +(\eta k_H^2)^3 \{ \text{cs}[\Gamma(\text{sc}, \text{ss}, \text{cc}) - \Gamma(\text{cc}, \text{ss}, \text{sc})] \\ &\quad - \text{cc}[\Gamma(\text{sc}, \text{cs}, \text{cc}) - \Gamma(\text{cc}, \text{cs}, \text{sc})] \} \\ a_{yy} &= -(\eta k_H^2)^3 \{ \text{cs}[\Gamma(\text{sc}, \text{sc}, \text{cs}) + \Gamma(\text{cc}, \text{cc}, \text{cs})] \\ &\quad + \text{ss}[\Gamma(\text{sc}, \text{sc}, \text{ss}) + \Gamma(\text{cc}, \text{cc}, \text{ss})] \} \end{aligned} \quad (\text{C3})$$

where

$$\begin{aligned} \Gamma(f, g, h) &= \\ &\int_0^\infty \int_0^\infty \int_0^\infty f(t-t')g(t-t'-t'')h(t-t'-t''-t''') \\ &\quad \exp[-\eta k_H^2(t'+2t''+t''')] dt' dt'' dt''' \end{aligned} \quad (\text{C4})$$

The combinations of trigonometric functions in (C3) can be expressed by the CC, CS, SC and SS defined in (19) and (31). In this way we arrive at the results (29) and (30).